

Nonlinear Deformation Analyses of Embankments on a Spatially Variable Liquefiable Deposit Modeled Using Conditional Random Fields

N. A. Paull, A.M.ASCE¹; R. W. Boulanger, F.ASCE²; and J. T. DeJong, M.ASCE³

¹Graduate Student Researcher, Dept. of Civil and Environmental Engineering, Univ. of California, Davis, 1 Shields Ave., Davis, CA 95616. E-mail: napaull@ucdavis.edu

²Professor, Dept. of Civil and Environmental Engineering, Univ. of California, Davis, 1 Shields Ave., Davis, CA 95616. E-mail: rwboulanger@ucdavis.edu

³Professor, Dept. of Civil and Environmental Engineering, Univ. of California, Davis, 1 Shields Ave., Davis, CA 95616. E-mail: jdejong@ucdavis.edu

ABSTRACT

Seismic evaluations of embankment dams and levees often involve synthesis and idealization of site investigation data in a simplified spatial structure with equivalent uniform properties assigned to each soil layer or category. The process of assigning equivalent single property values to entire soil layers and categories significantly simplifies the detailed information obtained during the site investigation. This study examines the potential benefits of incorporating the spatial variability of liquefiable soils captured in site investigation data into nonlinear deformation analyses (NDAs) of embankment dams using conditional random fields. Parent models (PMs) are analyzed using unconditional random fields to represent “true” subsurface conditions of a spatially variable, liquefiable soil layer under different size embankments. From each parent model, single continuous columns of soil data are extracted and used to simulate data obtained during site investigations. Conditional embankment models are created using random fields conditioned on the simulated site investigation data to represent possible subsurface conditions. Deformations obtained from sets of conditional model NDAs are compared to those obtained from their parent model NDAs for different embankment sizes and scales of fluctuation to examine the deformation prediction ability of the conditional models.

INTRODUCTION

A few prior studies have utilized stochastic random fields in nonlinear deformation analyses (NDAs) to assess potential seismic deformations of embankment dams. Boulanger and Montgomery (2016) conducted 2D NDAs of a 45 m high embankment dam on uniform and stochastic realizations of Standard Penetration Test (SPT) (N_1)_{60cs} values in an alluvial foundation layer. Their analyses concluded that utilizing uniform models with (N_1)_{60cs} ranging from the 33rd to the 50th percentiles would produce similar deformations as the stochastic models. Paull et al. (2019) conducted 2D NDAs of 5 m to 45 m high embankment models, and concluded that the representative percentile for (N_1)_{60cs} values increased with increasing normalized scale of fluctuation ($NSF_x = \theta_x / B$, where θ_x =horizontal scale of fluctuation and B =embankment base length) for the models tested with NSF_x between 0 and 0.8. These results are consistent with

those for other geotechnical systems (Baecher and Ingra 1981, Fenton and Griffiths 2008) that showed there was a critical correlation length of approximately 1B or 2B where stochastic models produce the largest standard deviation of deformations. Uncertainty in the estimated deformations depends on the extent and location of what is known about the site, and therefore, analyses conditioned on site exploration data may provide a potential to decrease the range of estimated deformations obtained from stochastic NDAs of embankment dams.

The current study examines the potential benefits of incorporating the spatial variability of liquefiable soils captured in site investigation data into nonlinear deformation analyses (NDAs) of embankment dams using conditional random fields. Parent models (PMs) are analyzed using unconditional random fields to represent “true” subsurface conditions of a spatially variable, liquefiable soil layer under different size embankments. From each parent model, single continuous columns of soil data are extracted and used to represent borehole data obtained during the site investigation. These simulated borings are then used to generate conditional realizations of the random field for the liquefiable soil layer. NDAs of several different sized embankment dams on the parent and conditioned, spatially variable, liquefiable soil layer are then performed. Sets of analyses with different embankment sizes and scales of fluctuation are utilized to compare their potential impacts on the deformation prediction ability of the conditional models. The deformation prediction ability of the conditional models are shown to depend on the NSF_x , the data used to condition the realizations, and the mode of deformation. This paper describes the NDA embankment models, the generation of parent and conditional realizations for the liquefiable soil layer, and the preliminary analysis results.

NDA MODELS AND PROCEDURES

Three different size embankments, shown in Figure 1, are analyzed using the 2D finite difference program FLAC 8.0 (Itasca 2016). The embankments are 10 m, 25 m, and 45 m tall with upstream slopes of 2.5:1 (H:V) and downstream slopes that varied from 2.5:1 near the crest to 3.5:1 near the toe. The alluvium layer is 12 m thick and the bedrock layer is 15 m thick (see Figure 1).

The procedures used to initialize the models and perform the dynamic analyses are described in Paull et al. (2019). Embankment models are created incrementally to approximate the construction process and establish the conditions at the time of ground motion shaking. The embankment shells are modeled using PM4Sand, and are assumed to be uniform. The alluvial layer is modeled using PM4Sand with properties based on correlations to the $(N_1)_{60cs}$ values from random fields (Boulanger and Ziotopoulou 2018). The core was modeled as a Mohr-Coulomb material with undrained shear strengths assigned using the procedure presented in Montgomery et al (2014). The bedrock was modeled as elastic with a shear wave velocity of 900 m/s. Stress conditions, including vertical and horizontal stresses, lateral earth pressure coefficient at rest (K_o) and initial static shear stress ratio (α) were checked to ensure reasonable initial stress and seepage conditions (Boulanger and Beaty 2016).

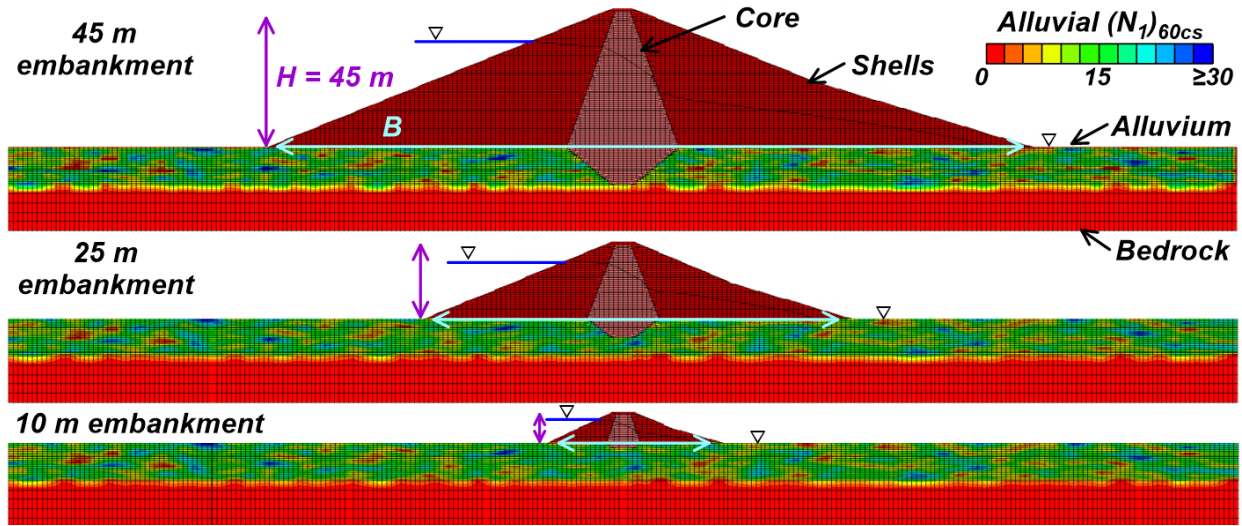


Figure 1. Embankment model geometries with the same unconditional realization of $(N_1)_{60cs}$ in the alluvial group (After Paull et al. 2019).

The PM4Sand model was calibrated following procedures recommended in Boulanger and Ziotopoulou (2018). The $(N_1)_{60cs}$ for the shells is set to 35. The $(N_1)_{60cs}$ for the alluvium are based on random fields, as described in the following section. The $(N_1)_{60cs}$ for each element is used to obtain relative density (D_R) and shear modulus coefficient (G_o) using correlations in Boulanger and Ziotopoulou (2018). The contraction rate parameter (h_{po}) for each element is selected based on single-element direct simple shear simulations to match the cyclic resistance ratio (CRR) based on the SPT based liquefaction triggering correlation from Boulanger and Idriss (2012). The remaining PM4Sand input parameters are kept at the default values.

All models are subjected to the TCU075 station east-west outcrop motion obtained from the NGA-West2 database (Ancheta et al. 2014), as recorded from the 1999 Chi-Chi earthquake ($M=7.6$) and scaled to a PGA of 0.6g. The outcrop ground motion is input as a shear stress time series to the compliant base of the embankment models based on the recommendations in Mejia and Dawson (2006). Free field conditions are applied to the lateral edges of each model with an equivalent elastic column of elements to maintain lateral confinement after liquefaction develops in the PM4Sand elements. A Rayleigh damping of 0.5% at a frequency of 3 Hz is used for all materials to provide a minimum level of damping in the small strain range for nonlinear materials and a nominal damping for the elastic bedrock material.

PARENT AND CONDITIONAL REALIZATIONS FOR ALLUVIUM

Parent models (PMs) were generated by spatially correlated, Gaussian random fields of $(N_1)_{60cs}$ values. The random fields were developed with a mean $(N_1)_{60cs}$ value of 15, a coefficient of variation (COV) of 40%, and truncated at a minimum $(N_1)_{60cs}$ value of 1.0 which affected less than 0.5% of the alluvial zones. The spatial correlation structure of the random fields is based on scales of fluctuation described in Vanmarcke (2010). The parent models are the same unconditional realizations presented in Paull et al. (2019).

Conditional realizations for the alluvium layer were generated using two approaches for considering continuous borehole data that might be collected along an embankment. The first approach was to consider only borehole data taken essentially at the location of the model cross-section (i.e., using only section-specific data). The second approach was to imagine that data obtained along the embankment length was used to generate site-wide statistical properties for the alluvium layer (e.g., mean and standard deviation), which are used in combination with the section-specific borehole/sounding data to constrain the conditional realizations. This paper will present results for analyses conditioned on borehole data taken from halfway up the upstream shell, halfway down the downstream shell and at the downstream toe in combination with site-wide statistics (i.e., the latter approach). Therefore, the conditional models in these analyses have the same overall statistical properties (mean, COV, scales of fluctuation) in the alluvial layer as their parent models.

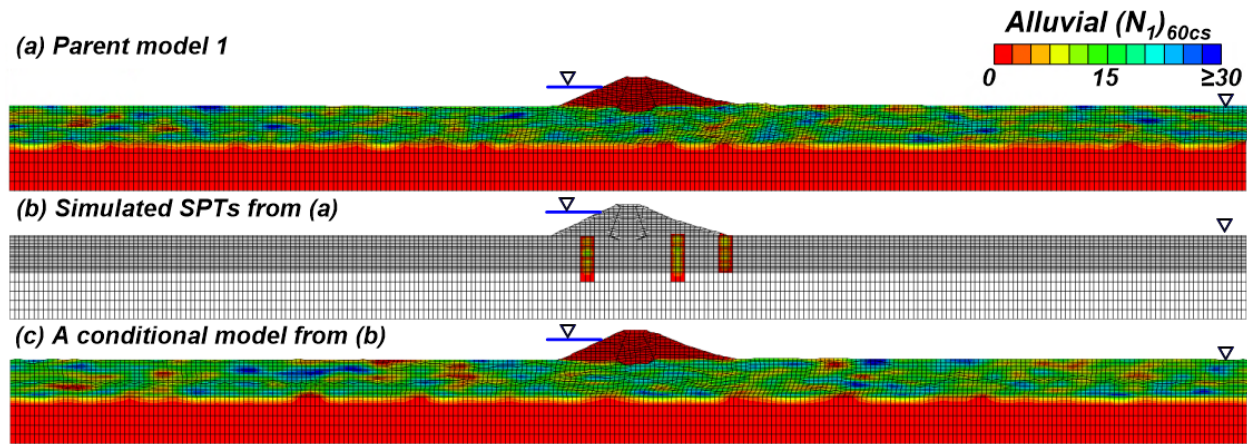


Figure 2. Deformed 10m embankment models: (a) unconditional PM 1, (b) simulated SPT columns extracted from (a), (c) a conditional model conditioned on the simulated SPT columns from (b).

ANALYSIS RESULTS

A comparison of the deformations obtained with the parent models and conditional models is used to assess the overall accuracy of the conditional models. In these comparisons, the parent models represent the “true” conditions, while the conditional models represent the “potential” conditions that could occur at the site given the site wide statistics and the section specific data. Therefore, for the conditional models to be accurate, they would produce deformations close to those for the “true” parent model. For these comparisons, normalized settlement (crest settlement normalized by the original embankment height) and normalized embankment stretch (horizontal stretch of the embankment toes normalized by the original embankment width) were chosen as appropriate deformation metrics to assess the accuracy of the conditional models. Sets of analyses with different size embankments and different horizontal scales of fluctuation to assess the effects of NSF_x on the deformation prediction ability of conditional models.

Comparison of different size embankments

Normalized deformations for the parent models and conditional models are shown in Figure 3. Each column of data points in Figure 3 shows a single parent model (green dot) and the related seven conditional models (blue dots) for the specified embankment height. The comparison of normalized deformations for different size embankments indicate that the conditional simulations often all produce deformations either larger or smaller than their parent models (PMs). For example, consider PM 3 and PM 5 for $H = 10$ m as shown in Figure 3a. The conditional models for PM 3 produce smaller and greater normalized crest settlements than the parent model, whereas the conditional models for PM 5 all produce greater normalized crest settlements than the parent model. Therefore, using a conditional model with the site wide statistics could under or over predict the normalized crest settlements for PM 3 whereas they would over predict normalized crest settlements for PM 5. The apparent bias in deformation estimates obtained using the conditional models for some parent models may be partly due to the small number of realizations and partly due to the characteristics of the simulated borehole data.

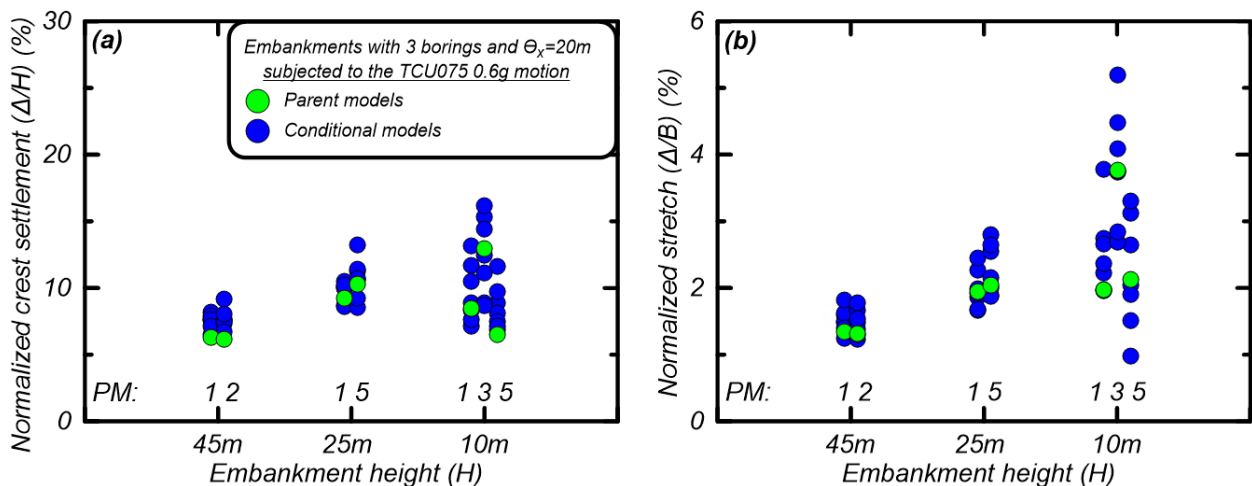


Figure 3. Normalized deformations of different size conditional embankment models and their PMs for (a) crest settlement and (b) embankment stretch.

The normalized deformations in Figure 3 show greater dispersion for the smaller embankment models than for the larger embankment models. The increased dispersion in normalized deformation for smaller embankments with the same alluvial statistics is due to the decreased averaging of soil properties along the deformation mechanism, which is consistent with Paull et al. (2019) and supports the use of NSF_x for these embankment model NDAs.

An assessment of the SPTs used to condition the analyses is conducted to assess the potential biases induced in the conditional models. For example, Figure 4 shows: (a) the cumulative distributions of PM 1 and the site investigation data to which three different size

embankment models were conditioned, and (b) profiles of the individual simulated borehole data. For the 10 m, 25 m, and 45 m high embankments, the cumulative distributions for the blow counts at the section of PM 1 are slightly smaller (by one or two blow counts) than the global distribution. Therefore, by conditioning the models to a decreased $(N_1)_{60\text{cs}}$ beneath the embankments, it is logical that the conditional models may deform more than the parent model.

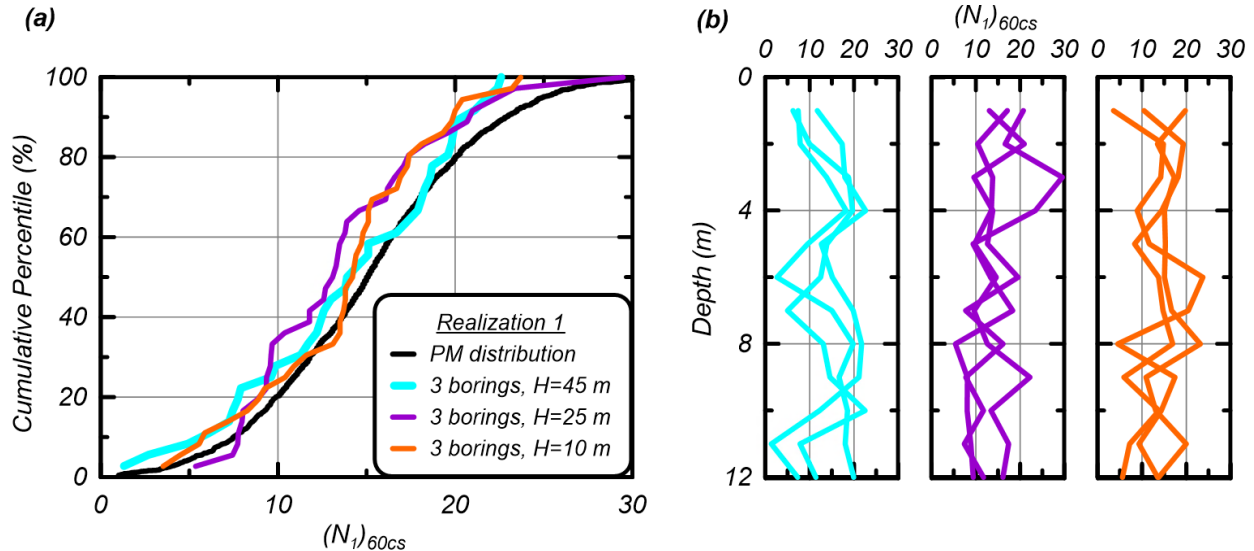


Figure 4. (a) Cumulative distributions of PM 1 and cumulative SPTs used for conditioning and (b) the simulated SPTs used for conditioning the 45 m, 25 m and 10 m conditional embankment models.

The results for the 10 m high embankment with other parent models show that sometimes the conditional models produce deformations smaller or greater than the parent model “true” deformations. For example, consider the normalized crest settlements (Figure 3a) for analyses based on PMs 3 and 5; conditional models for PM 3 gave some smaller and some larger deformations than the parent model, whereas conditional models for PM 5 tended to give greater deformations than the parent model. The borehole data for these two PMs are shown in Figure 5. For these cases, the cumulative distributions of the borehole data are not so different compared to the parent model distributions. Despite the similar cumulative distributions in borehole data, the crest settlement and embankment stretch for PM 3 are about double those for PM 5.

PM 5 produces less normalized settlements than the conditional models but comparable normalized embankment stretches (see Figure 3). For this case, it is expected that the parent model would produce less deformations than the conditional models due to the low blow counts in the conditioning borings, however, since the normalized embankment stretches both over estimate and under estimate the parent model, this behavior is primarily attributed to the specific locations of stronger and weaker areas. Closer examination of the deformation patterns for the

conditional models (see Figure 6) indicate that: (1) the conditional analyses produce greater settlements due to the presence of weaker locations within a few meters of the bottom of the core, and (2) the conditional analyses produce greater embankment stretches in cases where the deeper weak locations connect to more nearby weak locations. Therefore, even if the site investigations detect a specific pocket, by not detecting nearby pockets for which the deformation mechanisms can propagate, the conditional models do not recreate the deformation mechanism in the same way as the parent model “truth” and may provide deformations that are either more or less than the parent model.

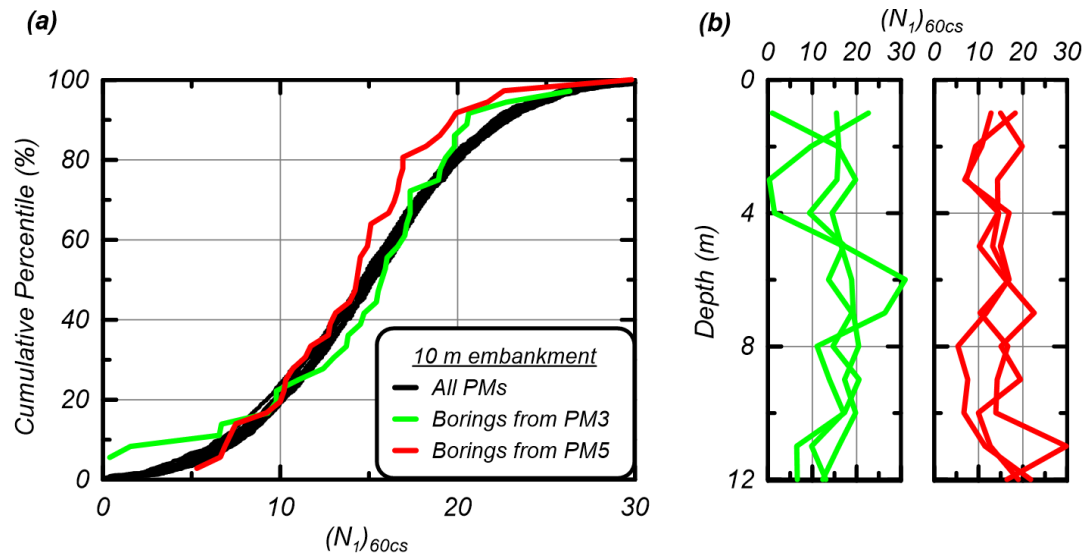


Figure 5. (a) Cumulative distributions of PMs 3 and 5 and cumulative borings used for conditioning and (b) the simulated SPTs used for conditioning the 10m conditional embankment models.

Comparison of different scales of fluctuation

The normalized deformations for both the PMs and conditional models of the 10 m embankment founded on material with three different scales of fluctuation ($\theta_x = 10$ m, 20 m and 60 m) were compared to assess potential effects of scale of fluctuation on the accuracy of the conditional models (Figure 7). The comparison of normalized deformations for different size embankments indicate that the conditional simulations often all produce deformations either larger or smaller than their PMs. The conditional models differed from the PMs by up to 12% for normalized settlement and 3% for normalized stretch for the embankment with a scale of fluctuation of 60 m. The largest differences were observed for the embankment models with a 60 m scale of fluctuation which generally has a larger range in normalized deformations. Along with the effects of the size of the embankment, these results support the use of NSF_x as an important parameter to consider when conducting NDAs of embankment dams.

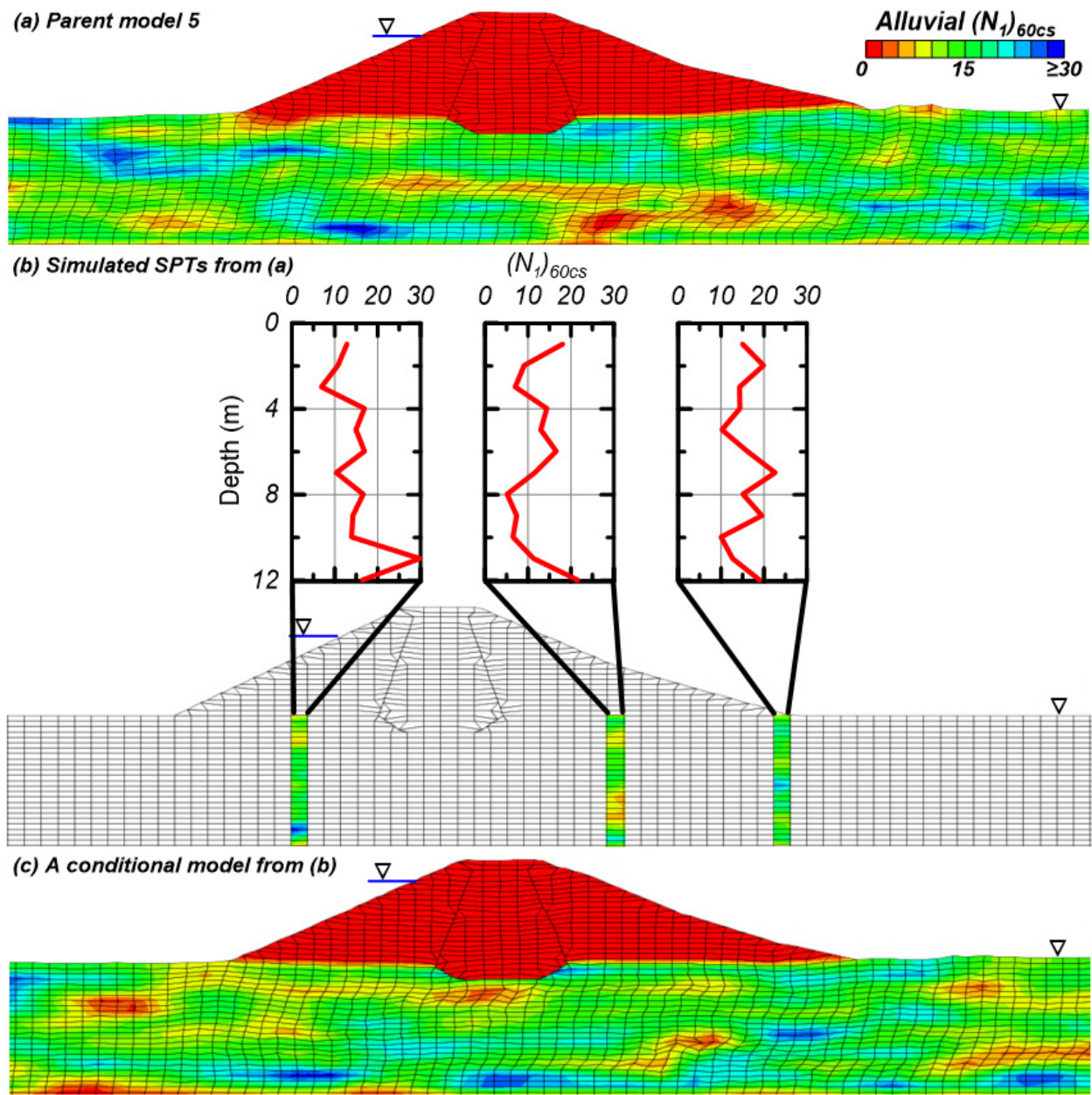


Figure 6. A section of deformed 10m embankment models: (a) Unconditional PM 5, (b) simulated SPT columns extracted from (a), (c) a conditional model conditioned on the simulated SPT columns from (b).

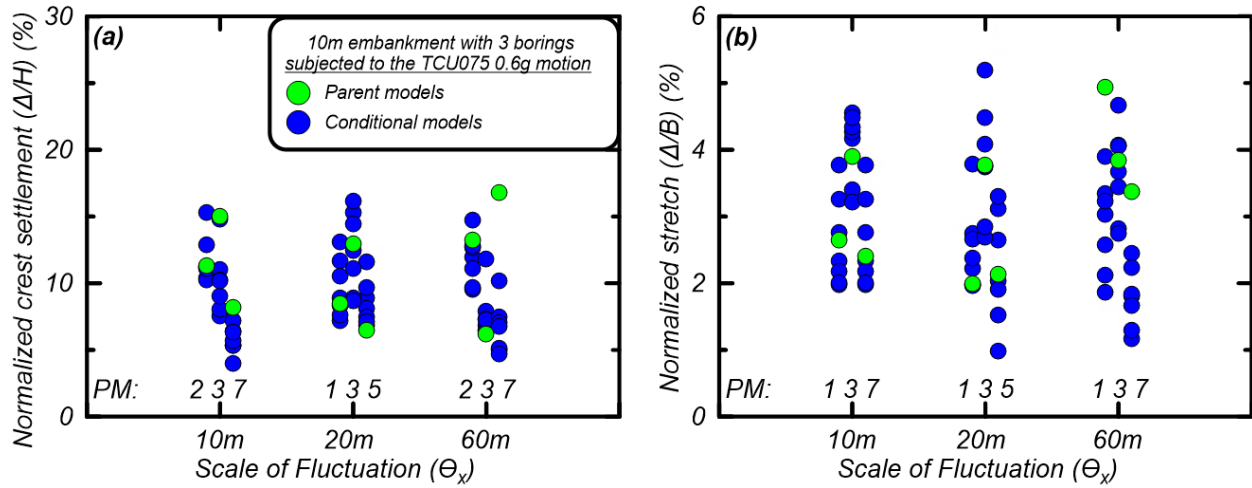


Figure 7. Normalized deformations of the 10 m conditional embankment model with different scales of fluctuation in the alluvial stratum and their PMs for (a) crest settlement and (b) embankment stretch.

CONCLUSIONS

The current study examines the effects of incorporating the spatial variability of liquefiable soils captured in site investigation data into nonlinear deformation analyses (NDAs) of embankment dams using conditional random fields. Parent models, for a spatially variable, liquefiable soil layer under an embankment dam are generated from unconditional random fields. From each parent model, columns of simulated soil data are extracted and used to represent site investigation data. These simulated SPTs are then used to generate conditional random fields for the liquefiable soil layer. NDAs with different embankment sizes and scales of fluctuation are utilized to compare their potential impacts on the deformation prediction ability of the conditional models. This paper describes the NDA embankment models, the generation of parent and conditional realizations for the liquefiable soil layer, and the preliminary analysis results.

The conditional model deformations are compared to their parent model “true” deformations to assess the potential accuracy of the conditional models. The conditional models may over or under predict the deformations of their parent models. Over or under predictions of displacements in the conditional models are often attributed to the borehole data: (1) having average (N_1)_{60cs} values that are smaller or greater than the true average below the embankments, or (2) missing an unusually large zone or cluster of zones of looser or denser materials that strongly influence computed deformations, particularly for smaller embankments. Therefore, if the normalized scale of fluctuation, NSF_x , within the liquefiable stratum is large enough that locally looser pockets do not average out with the surrounding denser zones, the identification of weak pockets during site investigations of the same stratum indicates the possibility for similar pockets to be located between site investigations and should be accounted for in an NDA of an embankment section. The range of normalized deformations are found to increase with increasing NSF_x , further supporting its use in assessing soil properties to be used in NDAs.

ACKNOWLEDGEMENTS

The work described herein progressed under projects for the California Division of Safety of Dams under Contract 4600009523, the Department of Water Resources under Contract 4600009751, and the National Science Foundation under grant CMMI-1635398. Any opinions, findings, conclusions, or recommendations expressed herein are those of the authors and do not necessarily represent the views of these organizations. The authors appreciate the above support.

REFERENCES

Ancheta, T. D., Darragh, R. B., Stewart, J. P., Seyhan, E., Silva, W. J., Chiou, B. S. J., et al.. (2014). NGA-West2 database. *Earthquake Spectra* EERI 2014; 30(3):989-1005.

Baecher, G. B., and Ingra, T. S., (1981). "Stochastic FEM in settlement predictions." *Journal of Geotechnical Engineering*, ASCE, 107(4), 449-464.

Boulanger, R. W., and Beaty M. H., (2016). "Seismic Deformation Analyses of Embankment Dams: A Reviewer's Checklist", In Proc., 36th USSD Annual Meeting and Conference, United States Society on Dams, 2016. 535-546.

Boulanger, R. W., and Idriss, I. M. (2012). "Probabilistic SPT-based liquefaction triggering procedure." *J. Geotechnical and Geoenvironmental Engrg*, ASCE, 138(10), 1185-1195.

Boulanger, R. W., and Montgomery, J. (2016). "Nonlinear deformation analyses of an embankment dam on a spatially variable liquefiable deposit." *Soil Dynamics and Earthquake Engineering*, 91, 222–233.

Boulanger, R. W., and Ziotopoulou, K. (2018). "PM4Sand (Version 3.1): A sand plasticity model for earthquake engineering applications." Report No. UCD/CGM-17/01, Center for Geotechnical Modeling, University of California, Davis, CA.

Fenton, G. A., and Griffiths, D. V. (2008). *Risk Assessment in Geotechnical Engineering*. John Wiley & Sons, Inc., New York.

Itasca (2016). *Fast Lagrangian Analysis of Continua (FLAC)*, release 8.0. Itasca Consulting Group, Inc., Minneapolis, MN.

Mejia, K. H., and Dawson, E. M. (2006). "4th International Symposium on Numerical Modeling in Geomechanics." Minneapolis, MN.

Montgomery, J., Boulanger, R. W., Armstrong, R. J., and Malvick, E. J. (2014). "Anisotropic Undrained Shear Strength Parameters for Nonlinear Deformation Analyses of Embankment Dams." *Geo-Congress 2014 Technical Papers*.

Paull, N. A., Boulanger, R. W., and DeJong, J. T., (2019). "Seismic deformations of different size embankments on a spatially variable liquefiable deposit", In Proc., 39th USSD Annual Meeting and Conference, United States Society on Dams.

Vanmarcke, E. (2010). *Random fields: analysis and synthesis*. World Scientific, Hackensack, NJ.

Ziotopoulou, K., & Boulanger, R. W. (2016). "Plasticity modeling of liquefaction effects under sloping ground and irregular cyclic loading conditions." *Soil Dynamics and Earthquake Engineering*, 84 (2016), 269-283, 10.1016/j.soildyn.2016.02.013.